



ELSEVIER

Thin-Walled Structures 40 (2002) 109–123

THIN-WALLED
STRUCTURES

www.elsevier.com/locate/tws

The influence of the fabrication process on the buckling of thin-walled steel box sections

Martin Pircher ^a, Martin D. O'Shea ^b, Russell Q. Bridge ^{a,*}

^aCentre for Construction Technology and Research, University of Western Sydney, Locked Bag 1797, South Penrith DC, NSW 1797, Australia

^bHyder Consulting Pty Ltd, Level 13, 601 Pacific Highway, St. Leonards, NSW 2065, Australia

Abstract

Steel box sections are usually fabricated from flat plates which are welded at the corners. The welding process can introduce residual stresses and geometric imperfections into the sections which can influence their strength. For some thin-walled sections, large periodic geometric imperfections have been observed in manufactured sections. Subsequent investigations have indicated that the imperfections are in fact buckling deformations i.e. the box section has buckled due to welding residual stresses prior to any application of external load. The welding procedure and the behaviour of the box sections under load has been modelled using a finite element analysis that accounts for both geometric and material non-linearities. Tests have been carried out on box sections with a range of width to thickness ratios for the plate elements. Modelling has been shown to give good correlation with the test results. The conditions for buckling to take place as a result of the welding process have been established. A design method has been proposed. © 2002 Elsevier Science Ltd. All rights reserved.

Keywords: Axial load capacity; Buckling; Design; Geometric imperfections; Residual stresses; Steel; Strength; Thin-walled box sections; Welding

1. Introduction

Thin-walled steel tubes filled with concrete form an economical solution for columns subjected to primarily axial loading. For economy reasons, a thin-walled steel section sufficient to carry the construction loading is provided while relatively inexpensive concrete is used as the major component to carry the design loading.

* Corresponding author. Fax: +61-2-4736-0833.
E-mail address: r.bridge@uws.edu.au (R.Q. Bridge).

Nomenclature

b	plate width
E_s	steel elastic modulus
f_{ol}	plate buckling stress
f_r	average compressive residual stress in plate
f_u	plate strength
f_y	steel yield stress
F_u	maximum axial force
k	plate buckling coefficient
L	length of box section
t	plate thickness
α	reduction factor for imperfections
λ_e	plate slenderness= $(b/t)(\sqrt{f_y}/\sqrt{250})$
λ_{ey}	plate yield slenderness limit
ν	Poisson's ratio

The strength of the steel tube is influenced by local buckling of the tube walls which is a function of the slenderness of the plate elements forming the tube. For rectangular or square bare steel tubes, the local buckling pattern can consist of inward and outward buckles and the influence of this local buckling on the column strength has been included in all major steel design specifications.

From the results of tests on thin-walled concrete filled tubes, Grimault and Janss [1] proposed an empirical effective area approach to account for observed local buckling effects. A theoretical study by Wright [2] of the elastic and inelastic buckling of plates in contact with a rigid medium, e.g. concrete, was empirically modified to determine plate slenderness limits for plastic, compact, semi-compact and slender plates. Nakai et al. [3] proposed an empirical relationship for the local buckling strength of steel tubes filled with concrete by assuming the plate elements to have all edges clamped. Some tests by Ge and Usami [4] indicated that this relationship was conservative. However, the plates were relatively stocky and the strength of the steel tube was determined by subtracting the strength of the concrete from the strength of the composite concrete–steel tube. Considering the variability of concrete and its compatibility with the steel tube, particularly where local buckling occurs, this procedure could be inaccurate. However, Han et al. [5] recently proposed a mechanics model for concrete filled SHS columns which considered the composite action between the SHS and the concrete.

Uy and Bradford [6] examined the elastic and inelastic local buckling of cold-formed profiled steel sheeting as used in composite profiled beams. They used the finite strip method to model the behaviour of thin plates against a rigid medium. This method is also applicable to concrete filled tubes.

Tests have been performed on cold-formed SHS to determine the yield plate slen-

derness limits where geometrical imperfections due to the cold forming process are insignificant [7–9]. In a paper by Bridge and O’Shea [10], the results of a series of tests on thin-walled square steel tubes with varying plate slenderness and varying length to width ratios have been reported. Two types of tests were performed for a range of combinations of plate slenderness and length: axial load on the bare steel tube; and axial load on the steel alone with un-bonded concrete in-fill to provide only lateral restraint. Residual stress measurements and plate imperfections resulting from the manufacturing process were also measured. The measured average compressive residual stresses f_r in the plate elements for the range of b/t ratios used in the test specimens are shown in Table 1 and the high values indicate the specimens were relatively heavily welded.

A number of these plate imperfection measurements indicated that some specimens displayed much greater deformations after fabrication than others. These imperfections were obviously introduced when the four flat plates representing the four sides of the box section were welded together to form the box. Comparing the residual stresses f_r and the buckling stress f_{oi} for each b/t ratio in Table 1 shows that for the specimens with b/t ratios of 130.7 and 112.1, the test residual stress f_r exceeds the buckling stress f_{oi} . This indicates that the stresses induced during the cooling of the four welds were enough to exceed the buckling resistance of the steel plates. Consequently, the measured high initial imperfections in these specimens were predominantly caused by buckling from the residual stresses.

Due to the great care that was taken to record the deformations and residual stress patterns after welding, a Finite-Element model of one of these specimens could be built where the recorded data was used for calibration. This FE-model and the influence of various geometric and material parameters on the local buckling under axial load were investigated.

2. The finite element model

2.1. Tube geometry

The measurements indicated that deformations and stress patterns were symmetric about the longitudinal plate centre-lines. Therefore only one quarter of the specimens

Table 1
Comparison of compressive residual stress and buckling stress

Specimen	b (mm)	b/t	Average residual stress f_r (MPa)	Buckling stress f_{oi} (MPa)
B24, 82×292 RES	80.0	37.3	153.3	554.2
B19, 122×568 RES	120.0	56.6	115.2	246.0
B22, 162×706 RES	160.0	74.7	103.1	138.3
B11, 202×706 RES	200.0	93.4	82.5	88.5
B2, 242×844 RES	240.0	112.1	63.3	61.4
B26, 282×982 RES	280.0	130.7	53.1	45.1

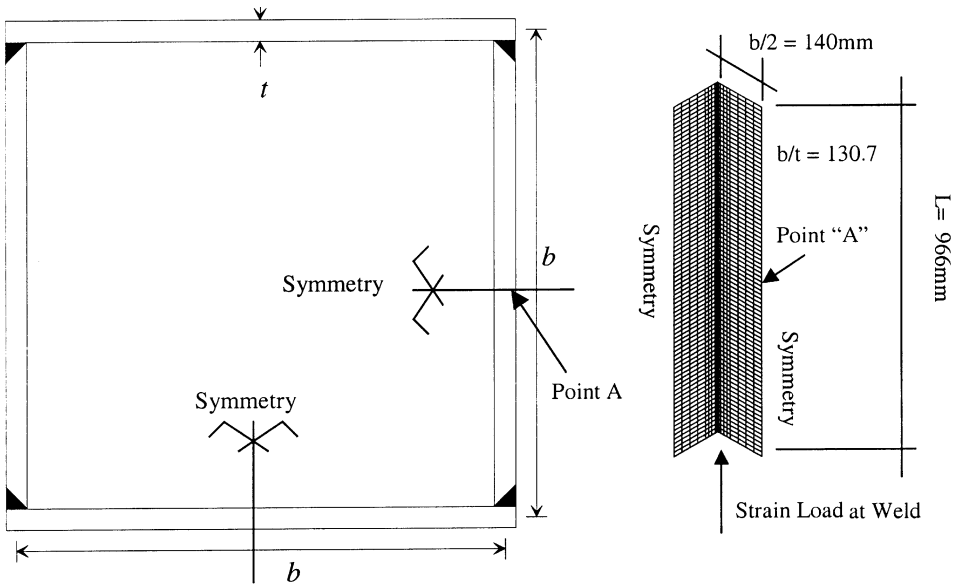


Fig. 1. Welded square steel tube—cross section and FE-model.

had to be represented in the FE-model as shown in Fig. 1. Fig. 1 also illustrates the dimensions of specimen ‘B27’ [10] used for the case study that is the basis for this paper.

2.2. Modelling the weld

In a preliminary study on the effect of welding on the behaviour of thin-walled shells [11], the cooling process of the weld was modelled taking into account the highly non-linear temperature dependent material properties of steel. The numerical results proved to be in close accordance with experimental results Fig. 2 but comput-

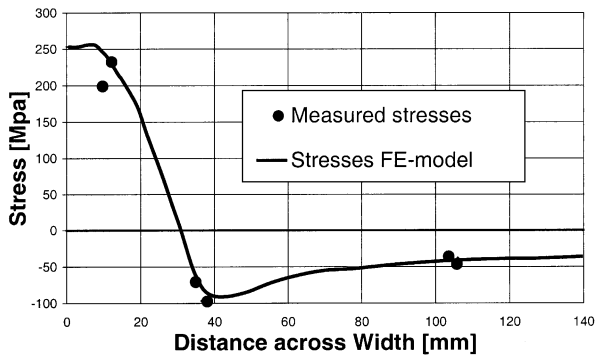


Fig. 2. Weld-induced residual stresses.

ing proved to be very expensive. An adaptation of a simplified procedure described by Rotter [12] proved to yield similar results. When using this method, a residual strain field is applied to the area around the weld. The applied strains cause deformations and residual stresses to form in a similar way as in the detailed model.

2.3. *Material properties*

To determine the steel material properties for the original test series [10,13], tension coupons were cut from a randomly selected steel sheet. These coupons were then tested in accordance with Australian Standard AS 1391 [14]. The final averaged steel properties were found to be $t = 2.142$ mm, $f_y = 282$ MPa and $E_s = 199,400$ MPa. In the computer analysis, two different simplified models were used and compared: firstly an elastic-plastic model; and secondly a bi-linear model which took strain hardening into account.

2.4. *Analysis*

A commercially available computer program called ABAQUS [15] was used. Fully integrated shell elements were employed. This software has been used previously in other research projects in the area of shell buckling [16] and found to give reliable results.

3. Test specimens

3.1. *Manufacture of test specimen and imperfection measurement*

All tubes were manufactured from mild steel sheets with a nominal thickness of 2 mm [10,13]. Four plates were cut from the sheet, tack welded into a box shape and then welded with a single bevel butt weld at the corners as shown in Fig. 1. The out-of-plane geometric imperfections of the tube walls after welding were measured on a grid on each face of the tubes using a Wild NA2 automatic level with a parallel plate micrometer. The results for the four faces of specimen B27, 282×928BS are shown in Figs. 3–6. The four sides were numbered clockwise 1–4 around the section as viewed from above. Residual stresses induced by the welding process were measured on a representative box using the sectioning technique. Strain gauges were placed at mid-height (cross section through the point ‘A’ in Fig. 1 on the internal and external faces. The complete set of measurements for geometric imperfections and residual stresses has been reported by O’Shea and Bridge [13].

3.2. *Testing procedure*

In the axial compression tests, the ends of the specimen were rotationally and laterally fixed by low temperature metal in a milled groove in custom built end plates. The specimens were tested under stroke control in a DARTEC 2000 kN

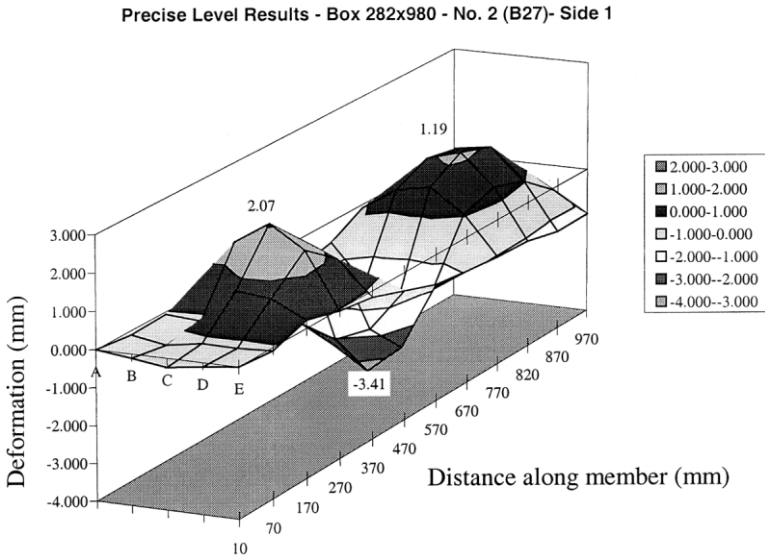


Fig. 3. Plate imperfection side 1, B27, 282×928BS.

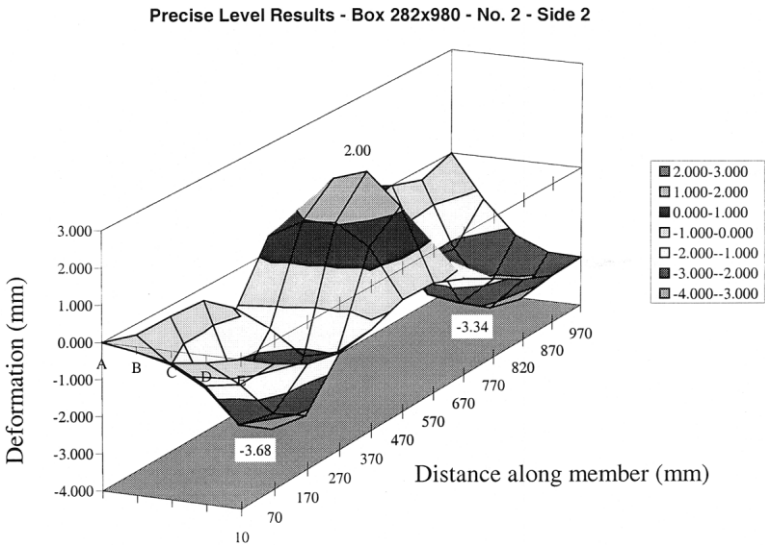


Fig. 4. Plate imperfection side 2, B27, 282×928BS.

testing machine. Axial shortening of the specimen was measured between thick machined plates using four linear displacement transducers evenly spaced around the specimen.

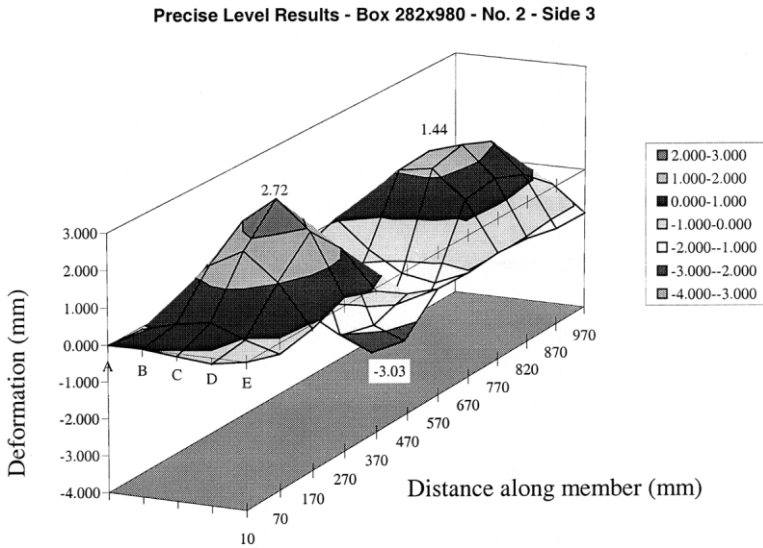


Fig. 5. Plate imperfection side 3, B27, 282×928BS.

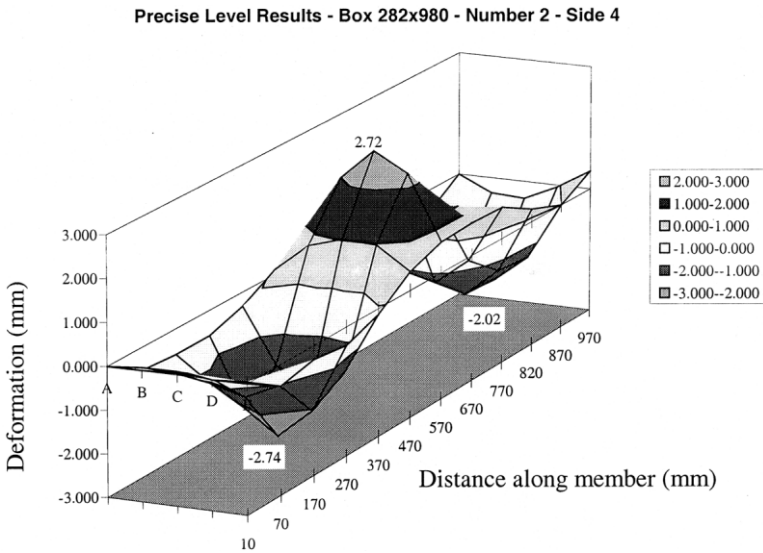


Fig. 6. Plate imperfection side 4, B27, 282×928BS.

4. Numerical study

4.1. Purely geometric imperfections

Only geometric imperfections were considered in a first series of analyses to separate the influences of geometric imperfections and weld-induced residual stresses on

Table 2
Results for various amplitudes of geometric imperfections

Imperfection amplitude in relation to wall-thickness	Maximum axial force F_u (kN)
10%	247.6
50%	242.1
100%	234.3
200%	224.7

the buckling behaviour. The shape of the first eigenmode under axial load was determined and superimposed onto the perfect shape of the box section. The amplitude of this imperfection was scaled to up to 2.0 wall-thicknesses (200%) and a buckling and post-buckling analysis under axial load was performed. The initial stiffness and the ultimate strength depended on the amplitude of the imperfection as listed in Table 2. Fig. 7 shows the load–displacement curves for these FE-models.

4.2. Weld shrinkage before load application

Residual stresses were taken into account in a second series of analyses. To produce a residual stress field matching measured results, strains were applied gradually along the welded zones. As the applied strains increased, the box sections responded linearly—tension stresses developed at the welded edges and pulled these edges outwards, inducing compressive stresses and small bending moments in the areas away from the weld which subsequently caused the sides of the box section to buckle. Fig. 8 shows the lateral deflection of Point ‘A’ (Fig. 1) in relation to the applied strains at the weld. During the pre-buckling phase only small deflections could be observed while the residual stress field developed to levels up to yield in tension at the welded edges. Strains applied after buckling had a great influence on the lateral displacements of the buckles but did not alter the residual stress patterns.

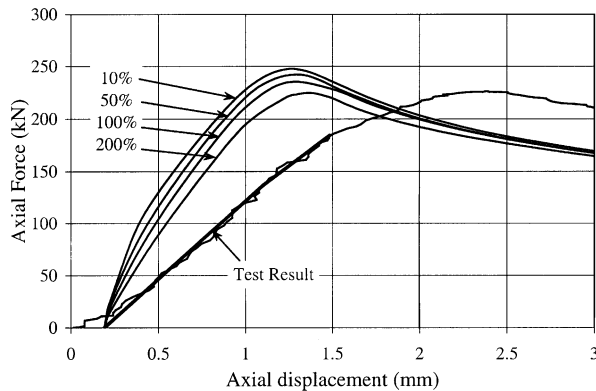


Fig. 7. Load–deflection curves—purely geometric imperfections.

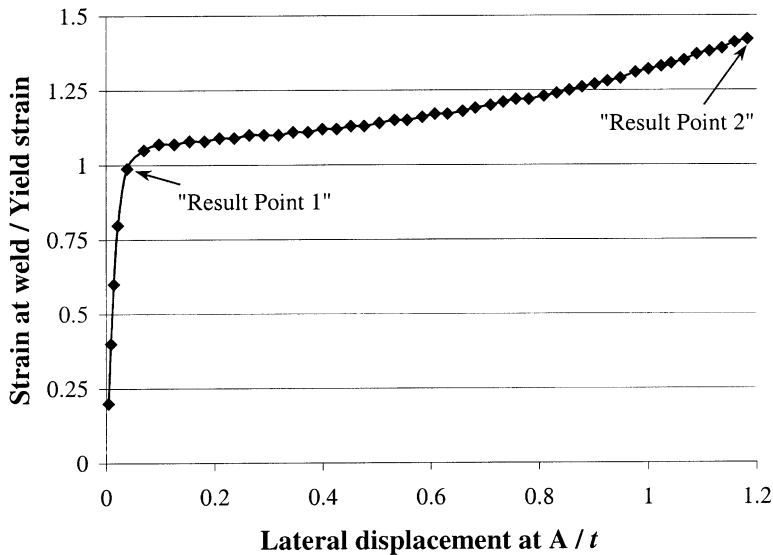


Fig. 8. Load–displacement curve for box sections under weld-induced strain loading.

4.3. Residual stresses and geometric imperfection

The amplitudes of the weld induced buckles measured in the test averaged 1.2 wall-thicknesses (120%). This value is reached at ‘Result Point 2’ (Fig. 8). At ‘Result Point 1’ (Fig. 8), the stress field is already fully developed but the amplitude of the geometric imperfections are only 0.1 wall-thicknesses (10%). These two points were used as a basis for ensuing analyses of the box under axial compression.

In Fig. 9, the influence of the residual stress field becomes apparent. The two curves marked stress-free in Fig. 9 are for box sections model imperfections of 1.2

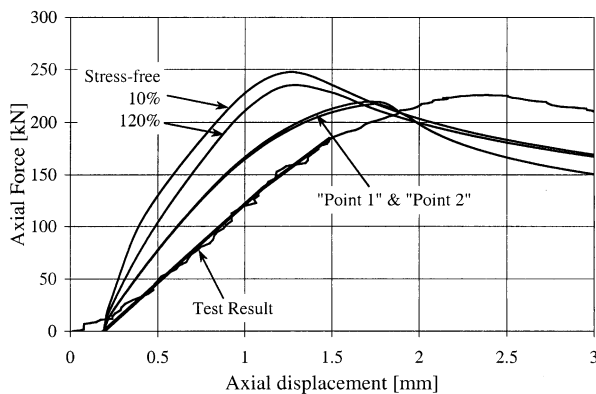


Fig. 9. Load–deflection curves—influence of residual stresses.

wall-thicknesses (120%) and 0.1 wall-thicknesses (10%) but with zero residual stresses (stress-free). As shown, the box with the larger 120% imperfection was less stiff and had a lower strength than the box with the 10% imperfection as might be expected. When the residual stresses are included (curves shown in Fig. 9 as Point 1 for 10% imperfection and Point 2 for the 120% imperfection), the stiffness and the ultimate strength of stresses are considerably lower than in the initially stress-free models. However, the amplitude of the geometric imperfection hardly influences the results when residual stresses are considered.

4.4. Boundary conditions

The results shown in Figs. 7 and 9 are for clamped boundary conditions modelling the boundary conditions during the experiments by O'Shea and Bridge [10,13]. The same analyses were repeated for simple supports. As illustrated in Fig. 10, using simply supported instead of clamped boundary conditions led to slightly lower ultimate loads and less stiffness in the pre-buckling phase.

4.5. Strain hardening

Elastic-plastic material behaviour was compared to a bi-linear material law which assumed first yield at 282 MPa and an ultimate stress of 374 MPa at a plastic strain rate of 0.6. These values correspond to those measured in the tension tests in [13]. Both material models resulted in the same weld-induced residual stress fields and displacements. Differences occurred in the post-buckling behaviour of the box where plastic hinges are developed and strain-hardening-reserves result in a significant gain in post-buckling strength Fig. 11. Again the amplitude of the initial geometric imperfection had hardly any effect on the load–deflection path of the structure.

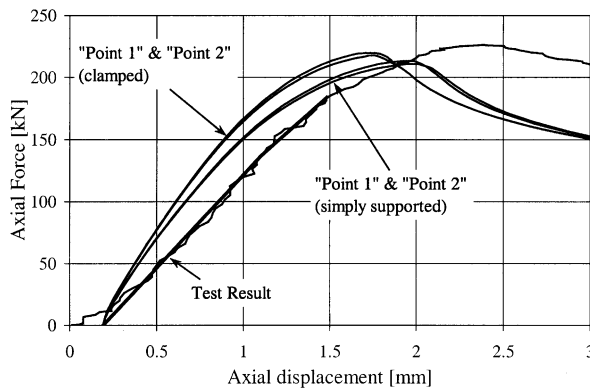


Fig. 10. Load–deflection curves—influence of boundary conditions.

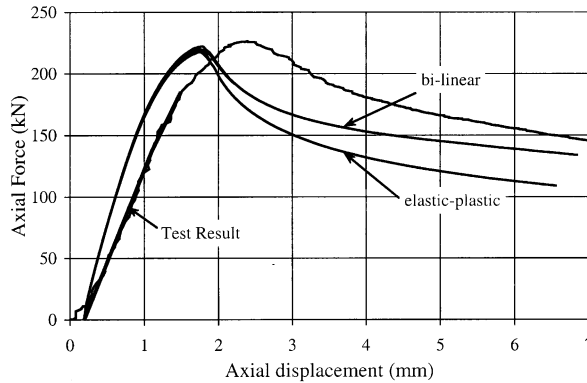


Fig. 11. Comparison of material models.

4.6. Comparison with laboratory test results

As can easily be seen in Fig. 7 and in Figs. 9–11, some differences exist between the measured results and the results gained from the computer models. The closest match was achieved when using the bi-linear material model. Pre-buckling stiffnesses still differed. An explanation can be found in the boundary conditions used in the tests. Rotations might not have been fully restricted and the low temperature metal holding the specimen in place might have had a softening effect. However, the ultimate loads and post-buckling behaviour in the FE-model closely resembled the results gained from the experiments [10,13]. Also, the computer model could generate the residual stress patterns and deflections caused by the cooling of the welds that were in very close accordance with the measurements [10,13].

5. Design recommendations

5.1. Local buckling

The local buckling stress f_{o1} for a rectangular plate subjected to uniaxial compression can be expressed as

$$f_{o1} = \frac{\pi^2 E_s}{12(1-\nu^2)} \frac{k}{(b/t)^2} \quad (1)$$

where E_s is Young's modulus of elasticity, ν is Poisson's ratio, b is the loaded width of the plate, t is the plate thickness and k is the buckling co-efficient which depends on the boundary conditions along the edges of the plate and the length L of the plate. For a long plate (large L) with all the edges simply supported (zero deflection but free to rotate), then $k = 4$. The hollow box section specimens [10,13] had an L/b ratio of 3.45 and were tested with fixed end conditions which corresponded to a value of $k = 4.27$ [10]. The box-section specimens with concrete infill have a differ-

ent buckling mode as inwards buckles are prevented. A finite strip analysis [10] was used to determine a numerical value of $k = 9.99$ for the test specimens which is similar to the value of $k = 32/3$ derived by Bradford, Uy and Wright [17] for long square box sections.

5.2. Design approaches

The design approach in the Australian Standard AS 4100 [18] is based upon an effective width concept developed by von Karman for perfect plates without residual stresses where the plate strength f_u is given by

$$\frac{f_u}{f_y} = \sqrt{\frac{f_{ol}}{f_y}} = \frac{26.88\sqrt{k}}{b/r\sqrt{f_y/250}} \quad (2)$$

using values of $E_s = 200,000$ MPa and $\nu = 0.3$ in Eq. (1) for the elastic buckling stress f_{ol} . The base value of yield stress used for designs to AS 4100 [18] is 250 MPa hence the use of the non-dimensionalised yield stress parameter $\sqrt{f_y/250}$. The von Karman expression in Eq. (2) has been modified in AS 4100 [17] by a reduction factor α to account for plate imperfections and residual stress such that

$$\frac{f_u}{f_y} = \alpha \sqrt{\frac{f_{ol}}{f_y}} = \frac{\alpha 26.88\sqrt{k}}{b/r\sqrt{f_y/250}} \quad (3)$$

Values for α , derived from the yield slenderness limits λ_{ey} in AS 4100 [18], are listed in Table 3 for plates with simply supported edges. For other plate edge boundary conditions, AS 4100 [18] assumes that the reduction factor α remains constant for a particular fabrication procedure and that the buckling coefficient k appropriate to the boundary conditions can be used in Eq. (3) to determine the strength f_u . For the welded box sections tested [10,13], the compressive residual stresses due to welding were in excess of 40 MPa (see Table 2) which is the upper limit in AS4100 [18] for lightly welded sections. Hence, these sections would be classified as heavily welded with a reduction factor $\alpha = 0.651$ (Table 3).

The design approach in AISI-LRFD [19] for a uniformly compressed stiffened elements (as in box sections) is based on the Winter formula where

Table 3
Strength Reduction Factors for AS 4100 [18]

Residual stresses	λ_{ey}	α
Stress relieved (SR)	45	0.837
Hot rolled (HR)	45	0.837
Lightly welded (LW)	40	0.744
Heavily welded (HW)	35	0.651

$$\frac{f_u}{f_y} = \sqrt{\frac{f_{ol}}{f_y} \left(1 - 0.22 \sqrt{\frac{f_{ol}}{f_y}} \right)} \tag{4}$$

which is similar to the approach used in AISC-LRFD [20] except that value of 0.22 is replaced by a value of 0.2.

The AS4100 von Karman and the AISI Winter design approaches are compared with the test results for the heavily welded hollow box sections (hollow squares) and similar filled box sections (filled squares) in Fig. 12. The test results in Fig. 12 have been plotted using the appropriate buckling coefficient for the specimens ($k = 4.27$ for the unfilled steel tubes and $k = 9.99$ for the unbonded filled steel tubes). It can be seen that the von Karman approach is conservative, particularly for the more slender box sections whereas the Winter approach is unconservative. O’Shea and Bridge [10] suggested a Modified Winter approach where

$$\frac{f_u}{f_y} = \left(\frac{f_{ol}}{f_y} \right)^{0.6} \left(1 - 0.25 \left(\frac{f_{ol}}{f_y} \right)^{0.6} \right) \tag{5}$$

The modifications to the exponent and the coefficient in the Winter formula are similar to those proposed by Kwon and Hancock [21] to account for distortional modes of buckling. The comparison with the test results in Fig. 12 shows the Modified Winter approach provides a better estimation of the strength of the specimens over the full range of plate slenderness.

6. Conclusions

A numeric study on the imperfections induced during manufacturing of bare steel tubes with a box cross-section was performed. Measured imperfections from a specimen of a laboratory test were reproduced in a computer analysis. This model was then

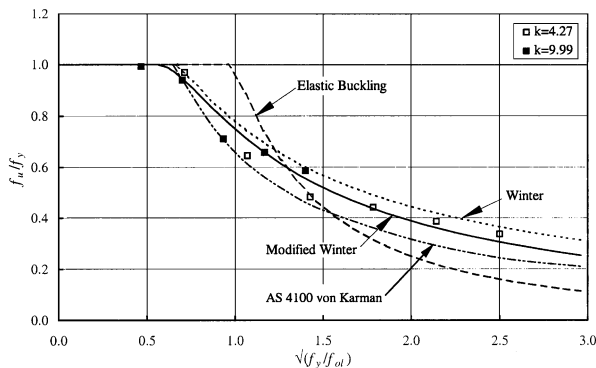


Fig. 12. Comparison of design approaches with test results.

used to perform a parameter analysis studying the influence of these imperfections on the buckling behaviour of this box under axial load.

It was shown that the amplitude of the imperfections effectively has no effect on the buckling strength, stiffness and post-buckling behaviour of the box when residual stresses are considered. However, when residual stresses are ignored and the buckling analysis is based on purely geometric imperfections, the amplitude of these imperfections has a strong influence on the response of the studied box.

Clamped end-supports were compared to simple supports and it was shown that clamping the ends of the box increases the stiffness and the ultimate strength by a small degree. Elastic-plastic material behaviour was compared to a bi-linear material model which accounts for strain-hardening and it was shown that using the bi-linear material law increased the post-buckling strength of the box. The response of the box in the laboratory test was matched closest by this computer model. Small differences between the numerical results and the test results could be explained by the softening effect of the implemented boundary conditions during the test program.

A modified Winter formula has been shown to provide close agreement with the test results for axially loaded heavily-welded thin-walled steel box sections with or without concrete infill provided the appropriate buckling coefficient is used in the formulation.

References

- [1] Grimault JP, Janss J. Reduction of the bearing capacity of concrete filled hollow sections due to local buckling. Preliminary report, ECCS Colloquium on Stability of Steel Structures, Liege, 1977:175–9.
- [2] Wright HD. Buckling of plates in contact with a rigid medium. *Structural Engineer* 1993;7(12):209–15.
- [3] Nakai H, Kitada T, Yoshikawa O. A design method of steel plate elements in concrete-filled square steel tubular columns. *Proceedings, Japan Society of Civil Engineers* I–3, 1985:405–13 [in Japanese].
- [4] Ge H, Usami T. Strength of concrete-filled thin-walled steel box columns: experiments. *ASCE Journal of Structural Engineering* 1992;118(11):3036–54.
- [5] Han LH, Zhao XL, Tao Z. Tests and mechanics model for concrete filled stub columns, columns and beam-columns. *Steel and Composite Structures—An International Journal* 2001;1(1):51–74.
- [6] Uy B, Bradford MA. Slenderness limits for thin steel plates restrained by concrete. In: *Proceedings, Australasian Structural Engineering Conference, Institution of Engineers Australia, Sydney, 1994:613–18.*
- [7] Key PW, Hasan SW, Hancock GJ. Column behaviour of cold-formed hollow sections. *Journal of Structural Engineering, ASCE* 1988;114(2):390–407.
- [8] Hancock GJ, Zhao XL. Research into the strength of cold-formed tubular sections. *Journal of Constructional Steel Research* 1992;23:55–72.
- [9] Zhao XL, Hancock GJ. Tests to determine the plate slenderness limits for cold-formed RHS of Grade C450. *Steel Construction, AISC, Sydney* 1991;25(4):2–16.
- [10] Bridge RQ, O’Shea MD. Behaviour of thin-walled steel box sections with or without internal restraint. *Journal of Constructional Steel Research* 1998;47(1–2):73–91.
- [11] Pircher M, Bridge RQ. Modelling the effects of a weld-induced circumferential imperfection on the buckling of cylindrical thin-walled shells. In: *Proceedings, Compumod Eleventh Annual Australasian Conference, Cairns, 1997: Paper 18.*
- [12] Rotter JM. Buckling and collapse in internally pressurised axially compressed silo cylinders with measured axisymmetric imperfections: imperfections, residual stresses and local collapse. In: *Proceedings, Imperfections in Metal Silos Workshop, Lyon (France), 1996:119–39.*

- [13] O'Shea MD, and Bridge RQ. Behaviour of thin-walled steel box sections with or without internal restraint. Research report R739. Sydney: School of Civil Engineering, University of Sydney, 1997.
- [14] Australian Standard. AS 1391-1991 method for tensile testing of metals. Sydney: Standards Australia, 1991.
- [15] Hibbitt, Karlsson, Sorenson. ABAQUS version 5.8-1 Standard Users Manual, Pawtucket (RI), 1998.
- [16] Pircher M, Bridge RQ. Buckling and post-buckling behaviour of silos and tanks under axial load—some new aspects. Engineering report CE18. Sydney: Centre for Construction Technology, University of Western Sydney, 2000.
- [17] Bradford MA, Wright H, Uy B. Local buckling of the steel skin in lightweight composites induced by creep and shrinkage. *Advances in Structural Engineering* 1998;2(1):25–34.
- [18] Australian Standard. AS 4100-1998 steel structures, Sydney: Standards Australia, 1998.
- [19] AISI-LFRD. Load and resistance factor design specification for cold-formed steel structural members. American Iron and Steel Institute, 1991.
- [20] AISI-LFRD. Load and resistance factor design: structural members, specifications and codes. American Institute of Steel Construction, 1994.
- [21] Kwon YB, Hancock GJ. Strength tests of cold-formed channel sections undergoing local and distortional buckling. Research report R640. Sydney: School of Civil and Mining Engineering, The University of Sydney, 1991.